一种新数值工具在车辆气动声学开发中的应用

PERUGINI Carlo Alberto[1]，ARZILLI Gilberto[2]，TORLUCCIO Antonio[2]，
BLUMRICH Reinhard[1]，WAGNER Andreas[1]

（1. Research Institute of Automotive Engineering and Vehicle Engines Stuttgart-FKFS，斯图加特 70596，德国；
2. Automobili Lamborghini S.p.A.，圣亚加塔·波隆尼 40019，意大利）

摘要：为了优化车辆开发过程的有效性，数值气动声学分析法的实施和应用对汽车制造商来说变得越来越重要。提出了一种结合延迟分离涡流模拟和基于Lighthill方程及声学扰动方程的有限元模型混合数值工具，应用 OpenFOAM 和 Actran软件实现了基于声学有限元法的近场声源区提取及声学压力脉动计算，并尝试应用于车顶扰流板及后视镜区域的气动噪声计算及分析。在兰博基尼 Urus 车型上，研究了不同车顶扰流板设计的气动声学行为，将仿真结果与斯图加特大学气动声学全尺寸风洞的实验结果进行比较，发现了令人信服的相关性。此外，探讨了扰流板上的主要噪声产生机制，研究了汽车表面压力波动水平随几何形状改变的变化情况。

关键词：车辆气动声学；计算气动声学；风噪；车辆舒适性
中图分类号：U462   **文献标志码**：A

Application of a Newly Implemented Numerical Tool for Aeroacoustic Vehicle Development

PERUGINI Carlo Alberto[1]，*ARZILLI Gilberto[2]*，*TORLUCCIO Antonio[2]*，*BLUMRICH Reinhard[1]*，*WAGNER Andreas[1]*

（1. Research Institute of Automotive Engineering and Vehicle Engines Stuttgart-FKFS，70596 Stuttgart，Germany；2. Automobili Lamborghini S.p.A.，40019 Sant'Agata Bolognese（BO），Italy）

Abstract：Nowadays，the implementation and application of numerical methodologies for aeroacoustic analysis become increasingly essential for car manufacturers in order to optimize the effectiveness of the vehicle development process. In this paper，a hybrid numerical tool based on the combination of a delayed detached eddy simulation and a finite element model was presented. The finite element model in turn was based on Lighthill's equation and acoustic perturbation equations. The computational fluid dynamics and the computational aeroacoustics were respectively performed by the software OpenFOAM and Actran. The aeroacoustic behavior of the SUV Lamborghini Urus using different roof spoiler designs was investigated. The numerical simulations were verified against the experimental measurements conducted in the aeroacoustics full scale wind tunnel of the University of Stuttgart operated by FKFS. Furthermore，the main noise generation mechanisms at the spoiler were discussed and the change of pressure fluctuation level on the car surface with respect to a geometry variation was investigated.

Key words：vehicle aeroacoustics；computational aeroacoustics；wind noise；vehicle comfort

Modern vehicles are expected to ensure the highest degree of safety and comfort. High interior cabin noise levels are no longer accepted and lead to annoyance of the passengers. Moreover，they may decrease the concentration of the driver. Depending on the tire-road combination，normally for passenger vehicles and for more or less constant speed above $100\sim120$ km/h，the overall interior noise level is driven by wind noise phenomena[1-2]. Under this perspective，the computational aeroacoustics（CAA）is nowadays important to face the above-mentioned criticalities[3]. It offers the advantage to provide a comprehensive set of data of the flow field not achievable by the limited capabilities of real experiments in a very early vehicle development phase. In view of these advantages the CAA，partly performed in parallel to wind tunnel experiments，has been proven to be promising with the prospect of cost reduction and the increase of effectiveness of the

entire vehicle development process. Several numerical approaches have been developed over the years[4-5]. However, the industrial applications need to find a trade-off between the accuracy of results and the required computational costs. Therefore, efficient numerical tools are needed to be embedded into the existing development process without compromising their efficiency. A two steps hybrid approach, relying on Lighthill's analogy[6], is widely used in industrial context in order to fulfill these demands. It combines a transient computational fluid dynamics (CFD) simulation, assuming incompressible fluid, and a finite element (FE) model[5,7-9]. In the first step, the velocity field around the car body is extracted. This velocity field is used by means of Lighthill's equation to calculate the aeroacoustic sources generated by turbulence and to subsequently solve the pressure fluctuations induced on the vehicle surface as shown for example in reference [7].

The present paper investigated the reliability, the accuracy, and the effectiveness of the exterior wind noise prediction performed by a hybrid approach newly implemented by FKFS and Automobili Lamborghini S. p. A. The CFD and the FE analysis (FEA) were performed by the software OpenFOAM and Actran, respectively. The SUV Lamborghini URUS at a speed of 140 km/h was used as the reference model for the investigations discussed in this paper. In the following section the numerical process and the related computational steps will be presented. Subsequently, the wind noise generation mechanisms of the roof spoiler will be discussed and the validation of the acoustic simulation results be presented. Lastly, an application of the considered numerical tool in a vehicle development scenario will be provided.

1　Numerical process

The considered numerical process consists of three main computational steps. First, an incompressible CFD simulation was performed in order to solve and extract the transient velocity field around the component of the vehicle (e. g. , side mirror, A-pillar, and roof spoiler) which is the subject of aeroacoustic investigations. Secondly, the velocity field, extracted by means of Lighthill's analogy, was used as the input for an FEA to compute the aeroacoustic sources in the same region. Lastly, the pressure fluctuations induced on the car surface were determined by using the same FE model to compute the exterior propagation. An overview of the process and the related software in use for each step is displayed in Fig. 1. For better understanding, a description of each step will be provided in the following sections.
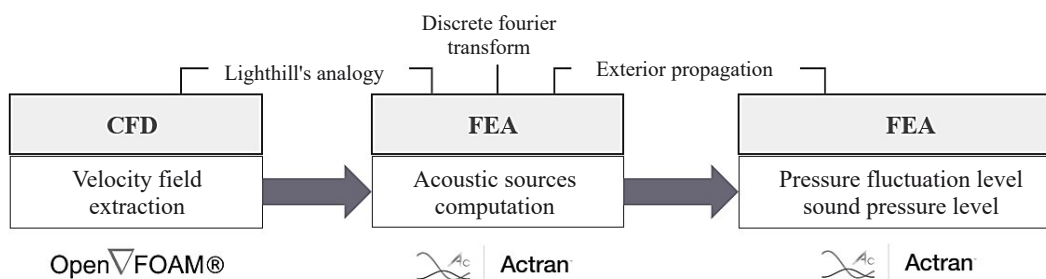

Fig.1　Workflow of CAA process

1.1　Velocity field extraction

A delayed detached-eddy simulation (DDES) with the Spalart-Allmaras turbulence model[10] is used in order to solve the transient flow field, assuming incompressibility of the flow. In Fig. 2 (left) an example of the extraction volumes involving the side mirror and the roof spoiler area, respectively, are provided. The CFD grid refinement is 3 mm, the time step used is 5×10^{-5} s, and the solution has been extracted for the duration of 0. 2 s. On the right-hand side of Fig. 2, a YZ-section of the velocity magnitude including the roof spoiler wake is shown as an example of the velocity field extracted around the roof spoiler.
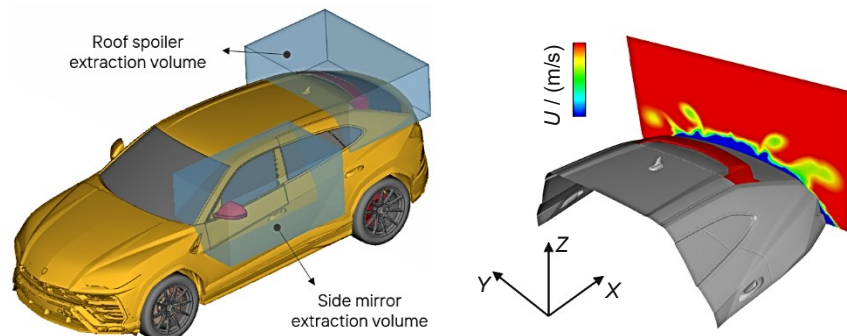
Fig.2　Velocity field extraction volumes for Lamborghini URUS (left) and velocity field behind the roof spoiler (right)

1.2　Acoustic sources computation

Different acoustic domains have been considered for the side mirror and the roof spoiler respectively, as shown in Fig. 3. The FE model of each domain has been divided in a source region (green) where the acoustic sources are solved and a buffer region (yellow) used to ensure the convergence of the numerical model and to adopt a non-reflecting boundary condition to the fluid boundary. In this latter region, no sources are calculated. Additionally, a reflecting boundary condition is assigned to the car surface. The acoustic sources are calculated by Actran performing the FE formulation of Lighthill′s analogy. A comprehensive explanation of the theory and the basics has been provided in reference[11] whereas the formulation used by the software Actran can be found in reference[12]. Moreover, a weighting function is applied in proximity to the source region boundary in order to smoothly attenuate the sources computed in this area. This spatial filter is used to avoid the generation of spurious noise sources due to the truncation effect by which the vortices crossing the source region border are affected. In Fig. 3 the acoustic domains used for the side mirror and the roof spoiler regions (left) and an overview on the FE mesh created for the roof spoiler (right) are presented.

After the computation of the acoustic sources, a Discrete Fourier Transform (DFT) is performed in order to convert the time domain into the frequency domain. DFT windows of 0.05 s have been used and the Hanning window function type has been applied with an overlap of 50% between each window.
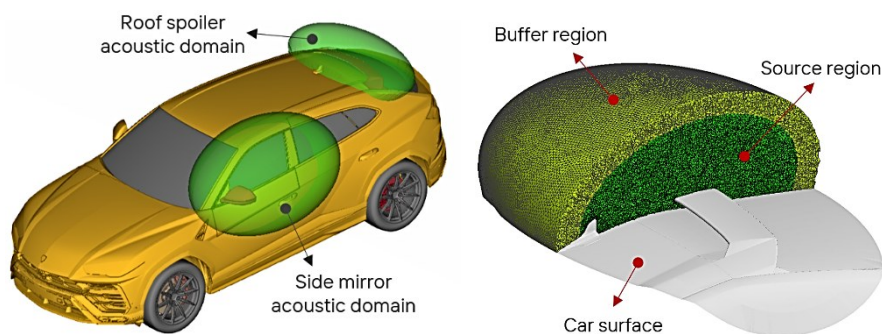

Fig.3　Acoustic domains around side mirror and roof spoiler (left) and FE model created for roof spoiler (right)

1.3　Pressure fluctuation level and sound pressure level

At this point of the process, the exterior propagation is performed in order to calculate the pressure fluctuation level (PFL) in the space and on the car surface. The PFL includes both the hydrodynamic as well as the acoustic contribution. By means of the acoustic perturbation equation (APE)[13],

which are based on the fact that acoustic fluctuations are characterized by large length scales and the hydrodynamic fluctuations by small length scales for same frequencies[12] , it is possible to separate the acoustic contribution from the hydrodynamic one. Hence, the sound pressure level (SPL) can be calculated by excluding the hydrodynamic part.

2　Discussion of results

The experimental investigations were conducted in the aeroacoustic full-scale wind tunnel of the University of Stuttgart, operated by FKFS. A closed cooling configuration of the car was used and, as usual for aeroacoustic standard measurements, all the sealings and gaps were fully taped in order to avoid unwanted sound sources. Furthermore, also as usual for aeroacoustic standard measurements the rotation of the wheels was neglected and no ground simulation system was used.

Following the structure of the simulation process, the validation was divided into two steps：
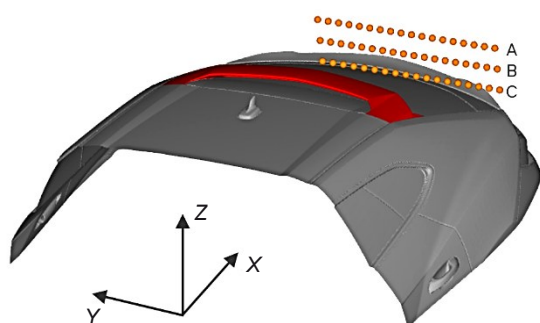
the validation of the velocity field solved by the CFD，and the validation of both the PFL and the SPL induced by the roof spoiler on the rear window and computed by the FE model. An overview of the main results is outlined below. In addition，an example of an application in a vehicle development scenario of the numerical process，that shows the aeroacoustic analysis of different spoiler design，is provided.

2.1　CFD validation

The velocity field was measured by using cobra probes from turbulent flow instrumentation (TFI) over a grid of 54 points placed on an YZ-plane, in the roof spoiler wake and perpendicular to the main flow direction (X) (see Fig. 4). The velocity magnitude, (U_{mag}) measured for each point of the grid, has been averaged over time and normalized by the free stream velocity (U_{inf}). In this way a direct comparison between wind tunnel measurements and CFD results has been carried out. For brevity, only the results related to the points belonging to the middle line B are reported in Fig. 4(right).
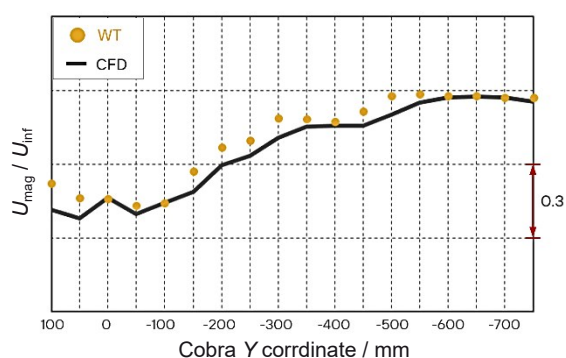

Fig.4　Velocity field measurement points (left) and velocity magnitude comparison between experiments and simulations for line B (right)

A good agreement between CFD and experimental results has been found. Averaging over the points of each line (A, B and C), the percentage errors obtained are lower than 6%. However, in the most turbulent regions some higher deviation between simulation and measurements is observed. In these areas many factors must be considered. Both, the CFD grid size and the turbulence model used can lead to inaccuracy in predictions. Moreover, due to its shape the multi-hole probe type used in the

measurements has limited capabilities in measuring velocity components in turbulent and highly separated regions with e. g. back-flow. All in all, the accuracy of the CFD modelling is considered to be suitable to use the velocity field as an input for the FE model.

2.2　FEA validation

The exterior noise investigation was carried out by analysing the SPL of the aeroacoustic sources around the roof spoiler region as well as by the analysis of the PFL induced on the rear window. The former

was measured by the FKFS microphone array system [14] and the latter by a set of surface microphones (B&K $\frac{1}{2}'$ type 4949) installed on the rear window as shown in Fig. 5.

The measurements highlight that the most critical acoustic sources are distributed along the leading edge of the spoiler and that the related SPL reaches its maximum in this area. The CAA prediction, in good agreement with the experiments, shows a consistent SPL distribution on the spoiler and car surface. The simulation results point out that the main noise generation mechanisms are mostly located between the lower part of the leading edge and the car rear window. Furthermore, it has been observed by steady Reynolds Averaged Navier Stokes (RANS) simulations that the top and the bottom part of the leading edge are both surrounded by flow with high turbulent kinetic energy (TKE) content. The TKE, and thus the noise generation mechanisms, seems to be especially related to a local separation occurring on the leading edge area and to the high turbulent wake generated by the antenna that impinges on the central part of the spoiler.
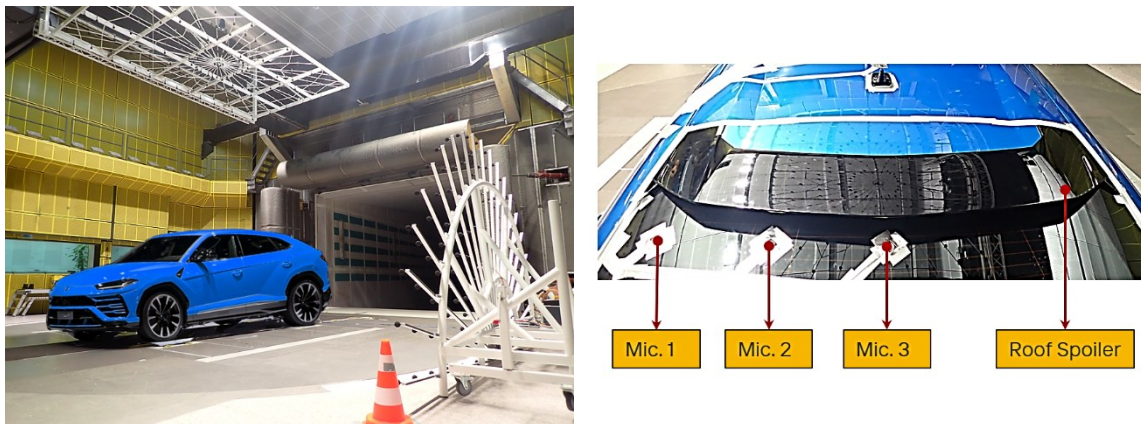

Fig.5　Microphone array in aeroacoustic wind tunnel (left) and first row of surface microphones on rear window (right)

The phenomenon discussed above, which is visible over the whole considered frequency range (here up to 2.5 kHz), is presented in Fig. 6 by a top view of the roof spoiler. Here, the SPL level determined by the microphone array is compared to the related simulation results. As an example, a third-octave band visualization with a central frequency of 1.6 kHz has been selected. Additionally, iso-surfaces of TKE colored by total pressure coefficient, calculated by a steady RANS simulation, are shown. This example shows that already the relatively low-cost RANS simulations can provide possible explanations of aeroacoustic phenomena.
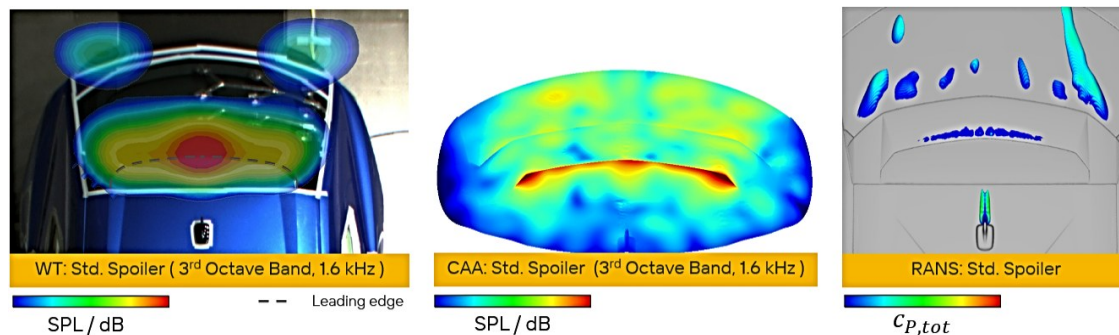

Fig.6　SPL measured by wind tunnel microphone array (left), SPL distribution around roof spoiler predicted by CAA (center) and iso-surface of TKE colored by total pressure coefficient predicted by RANS (right)

In order to validate the local PFL in the simulation results on the rear window, the above-mentioned surface microphones shown in Fig. 5 were used. The comparison between simulation and measurement can be seen in Fig. 7. The PFL predicted by the CAA (red/thick line) is very consistent to the experiments (black/ thin line) up to 1. 2 kHz for the microphones 1 and 3, and up to 2. 5 kHz for microphone 2. However, the experiments and the simulations are characterized by different fluctuation amplitudes. This is due to the different time windows used for the two analyses considered：20 s for the experiments and a more restricted window of 0. 2 s for the simulations due to the high computational cost involved. The deviation from the measurements occurring beyond 1. 2 kHz can be explained by the limitation in turbulence prediction of the DDES simulation which has been performed here (to save computational costs at this stage). As explained in reference ［3］, according to the applied grid only part of the turbulence scales is solved, whereas the remaining part related to the smaller scales is modelled. Therefore, the flow field solved in the first part of the process is characterized by a cut-off frequency determined by the size of the CFD grid used. For a better understanding, the sensitivity analysis of the CFD mesh size related to the PFL prediction will be the subject of further investigations.
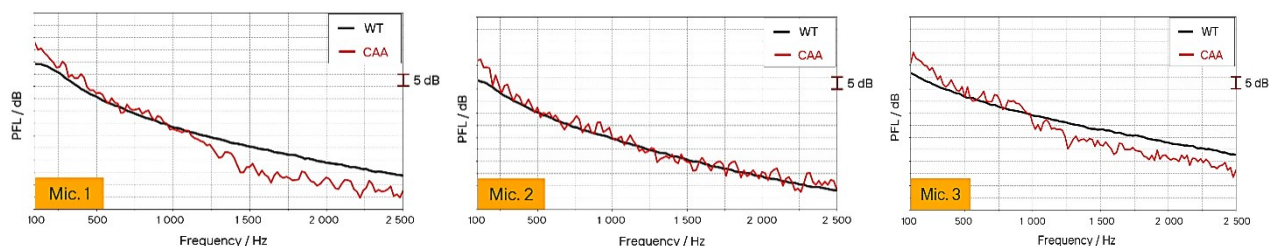

Fig.7　Pressure fluctuation level on rear window: wind tunnel measurements (WT) versus CAA

2.3　Application in vehicle development

The numerical tool has been used to analyze the acoustic behavior of two different roof spoiler designs：standard (illustrated in Fig. 5) and variant. The predicted PFL distribution on the rear window has been compared to an interior cabin noise investigation carried out during the wind tunnel experiments and road tests. During the wind tunnel sessions, the interior SPL has been measured by artificial heads located on the rear passenger seats and the related articulation index has been calculated. Moreover, the articulation indices for the same spoiler configurations were calculated during road test by using a microphone located also on the rear seats of the cabin. In Fig. 8 the interior SPL measured by wind tunnel experiments and the articulation indices evaluated during wind tunnel as well as road tests for both the standard (dark green) and the variant (black) spoiler is presented.

The artificial head measurements highlight a significant decrease of the broadband noise due to the installation of the standard spoiler. Furthermore, the mentioned spoiler configuration leads to an increase of the articulation index of 7％ during wind tunnel sessions and of 5％ as reported by road test data. Both the interior noise experimental analysis show that the standard spoiler leads to an overall acoustic improvement compared to its variant. The CAA process, implemented so far for exterior aeroacoustics investigations, has also been found to be consistent with the interior noise analysis mentioned above. The contrasting acoustic behavior, caused by the different spoiler designs installed, is well predicted by the exterior acoustic analysis performed by the aeroaocustic simulations. As can be seen in Fig. 9, the PFL distribution on the rear window induced by the standard spoiler points out a significant load decrease compared to its variant consistently to the interior noise reduction shown by the previous experimental investigation.
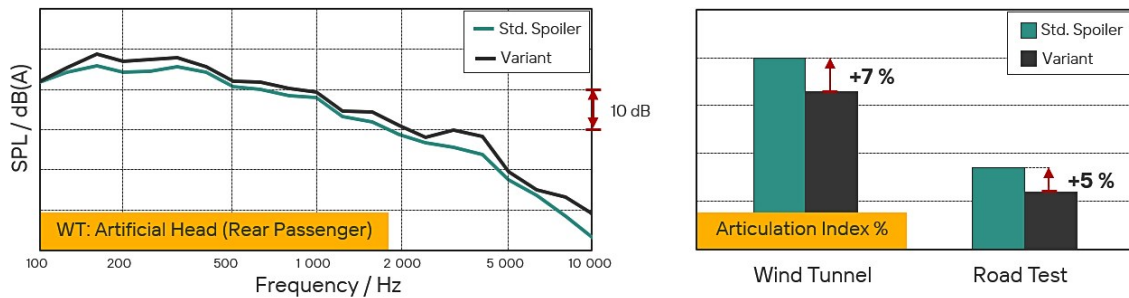
Although the mere exterior investigation does

Fig.8 Interior cabin SPL measured by artificial head (left), articulation index reported by wind tunnel and road test (right) for standard spoiler and variant design

not ensure a correct evaluation of the cabin noise behavior, the provided example shows that the numerical process newly implemented provides high potential with respect to aeroacoustic predictions. It

also shows in which way it can be embedded as an additional tool, in parallel with the wind tunnel experiments and the road tests, in the vehicle development process.
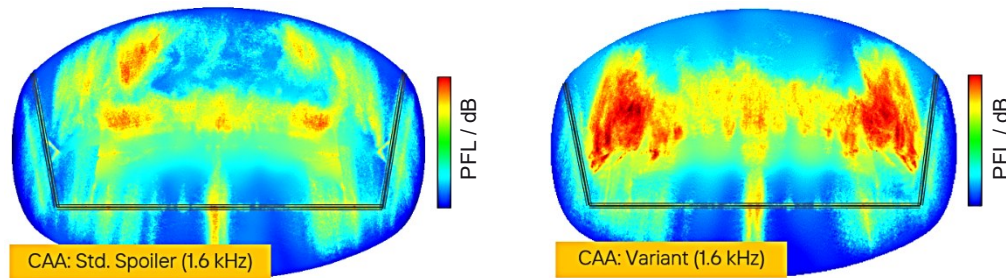

Fig.9 PFL distribution on rear window predicted by CAA for standard spoiler design (left) and variant design (right)

3 Conclusions

The newly implemented numerical tool, consisting of the combination of a delayed detached eddy simulation and a finite element model has shown convincing correlations to the experiments. The combined validation of the CFD simulations and the FE analysis has proven the robustness of the whole numerical tool implemented for exterior aeroacoustic investigations. Furthermore, the computational cost of the presented hybrid process, not discussed in this paper, and the accuracy of the predictions with respect to the exterior, as well as the agreement in tendencies with the interior noise experiments, have been found to be suitable for industrial applications. Therefore, this newly implemented numerical process can be considered being an efficient tool, embeddable in the vehicle development process in order to optimize its performance in terms of costs and effectiveness. Further investigations will focus on

the implementation of an additional computational step regarding the interior noise propagation. Combining among others the PFL distribution, calculated on the windows of the vehicle, and the eigenmodes of the same windows, it will be possible to simulate the noise transmission into the cabin and therefore the SPL at the ears of the passengers.

References:

[1] SCHÜTZ T. Hucho-aerodynamik des automobils [M]. Wiesbaden: Springer Fachmedien Wiesbaden, 2013.

[2] OETTLE N, SIMS-WILLIAMS D. Automotive aeroacoustics: An overview[J]. Proceedings of the Institution of Mechanical Engineers Part D Journal of automobile engineering, 2017, 231(9): 1177.

[3] TAM C K W. Computational aeroacoustics: Issues and methods[J]. AIAA Journal, 1995, 33(10): 1788.

[4] MARBURG S, NOLTE B. Computational acoustics of noise propagation in fluids-finite and boundary elements methods [M]. Berlin Heidelberg: Springer, 2008.

[5] MANOHA E, REDONNET S, CARO S. Computational

Aeroacoustics［J］. Encyclopedia of Aerospace Engineering，2010.

［6］ LIGHTHILL M J. On sound generated aerodynamically［J］. Proceedings of the Royal Society，1952. DOI：10.2307/2414246.

［7］ PIETRZYK A，BESKOW D，MOROIANU D，*et al*. Passenger car side mirror exterior noise simulation and validation［C］// The 22nd International Congress on Sound and Vibration. Florence：［s. n.］，2015.

［8］ CARO S，PLOUMHANS P，GALLEZ X. Implementation of Lighthill's acoustic analogy in a finite/infinite elements Framework ［C］// 10th AIAA/CEAS Aeroacoustics Conference. Manchester：American Institute of Aeronautics and Astronautics，2004.

［9］ CARO S，DETANDT Y，MANERA J. Validation of a new hybrid CAA strategy and application to the noise generated by a flap in a simplified HVAC duct［C］// 15th AIAA/CEAS Aeroacoustics Conference，Miami：American Institute of Aeronautics and Astronautics，2009.

［10］ SPALART P R. Detached-eddy simulation［J］. Annual Review of Fluid Mechanics，2009，41：181.

［11］ OBERAI A A，ROKNALDIN F，HUGHES T J R. Computational procedures for determining structural-acoustic response due to hydrodynamic sources［J］. Computer Methods in Applied Mechanics and Engineering，2000，190(3/4)：345.

［12］ Free Field Technologies SA. ACTRAN 2020 user's guide - Volume 1［Z］.［S. l.］：Free Field Technologies SA，2019.

［13］ EWERT R，SCHRÖDER W. Acoustic perturbation equations based on flow decomposition via source filtering［J］. Journal of Computational Physics，2003，188(2)：365.

［14］ RIEGEL M，BLUMRICH R，MINCK O，*et al*. New large microphone array at the FKFS wind tunnel［C］// 12th FKFS-Conference Progress in Vehicle Aerodynamics and Thermal Management. Stuttgart：FKFS，2019.